THE JOURNAL OF BIOLOGICAL CHEMISTRY
Vol. 263, No. 32, Issue of November 15, pp. 16954-16962, 1988
Printed in U.S.A.

Native Mitochondrial Creatine Kinase Forms Octameric Structures

II. CHARACTERIZATION OF DIMERS AND OCTAMERS BY ULTRACENTRIFUGATION, DIRECT MASS MEASUREMENTS BY SCANNING TRANSMISSION ELECTRON MICROSCOPY, AND IMAGE ANALYSIS OF SINGLE MITOCHONDRIAL CREATINE KINASE OCTAMERS*

(Received for publication, March 23, 1988)

Thomas Schnyder‡, Andreas Engel§, Ariel Lustig¶, and Theo Wallimann‡‖

From the ‡Institute for Cell Biology, ETH-Hönggerberg, CH-8093 Zurich, Switzerland, and the §Maurice E. Müller Institute for High Resolution Electron Microscopy and the ¶Departement of Biophysics, Biocenter, University of Basel, Klingelbergstrasse 70, CH-4056 Basel, Switzerland

Electron micrographs of negatively stained and metal-shadowed mitochondrial creatine kinase (Mi-CK) molecules purified as described by Schlegel *et al.* (Schlegel, J., Zurbriggen, B., Wegmann, E., Wyss, M., Eppenberger, H. M., and Wallimann, T. (1988) *J. Biol Chem.* 263, 16942–16953) revealed a homogeneous population (≥95%) of distinctly sized square-shaped, octameric particles with a side length of 10 nm that frequently exhibited a pronounced 4-fold axis of symmetry. The cube-like molecules consist of four dimers that are arranged around a stain-accumulating central cavity of 2.5–3 nm in diameter. This interpretation is supported by single particle averaging including correlation analysis by computer. Upon prolonged storage or high dilution, the cube-like octamers tended to dissociate into "banana-shaped" dimers.

Sedimentation velocity and sedimentation equilibrium experiments yielded an *s* value of 12.8–13.5 S and an M_r of 328,000 ± 25,000 for the octameric cubes. An *s* value of 5.0 S and a M_r of 83,000 ± 8,000 was found under conditions which revealed banana-shaped dimers. These dimers proved to be very stable, as their dissociation into monomers of 45 kDa (*s* value = 2.0 S) required 6 M guanidine HCl. Thus, the oligomeric structures observed in the electron microscope are identified as Mi-CK dimers (banana-shaped structures) and cubical Mi-CK octamers assembled from four Mi-CK dimers.

The octameric nature of native Mi-CK and the formation of Mi-CK dimers were confirmed by direct mass measurements of individual molecules by scanning transmission electron microscopy yielding a molecular mass of 340 ± 55 kDa for the octamer and 89 ± 27 kDa for the dimer.

A structural model of Mi-CK octamers and the possible interaction with ATP/ADP-translocator molecules as well as with the outer mitochondrial membrane is proposed. The implications with respect to the physiological function of Mi-CK as an energy-channeling molecule at the producing side of the phosphoryl creatine shuttle are discussed.

Native mitochondrial creatine kinase (Mi-CK)[1] purified by the rapid method described in the preceding publication (1) exhibits the biochemical characteristics of a homogeneous high molecular weight polymeric form of 360,000 ± 30,000 that consists of four Mi-CK dimers with two identical subunits of a M_r of 42,000–43,000 each as determined by gel permeation chromatography and sodium dodecyl sulfate-gel electrophoresis.

Thus, besides its specific localization restricted to mitochondria (1–3), Mi-CK forms highly ordered octameric structures that are unique for Mi-CK and have never been found with BB-CK or MM-CK isoforms from brain or muscle, respectively. The latter two isoforms only form dimeric structures with a M_r of approximately 80,000–85,000 (4). In addition, Mi-CK differs from the B- and Mi-CK subunits in amino acid composition (5, 6), amino acid sequence (7), and immunological properties (8) and is encoded by separate Mi-CK gene(s) (7). Mi-CK is found in tissues of sudden high energy demand, *e.g.* in mitochondria from cardiac and skeletal muscle, brain (3, 9), spermatozoa (10, 11), and photoreceptor cells of retina (12). So far, Mi-CK has always been found in conjunction with one of the other CK isoforms which had been considered in the past to be exclusively cytosolic or "soluble" enzymes. However, a respectable body of data has been accumulated over the past 10 years showing that small, but functionally significant, fractions of B- or M-type CK isoforms are localized at specific intracellular sites of high ATP demand, *e.g.* at the myofibrillar M-band (13–15), at the acetylcholine-receptor-rich membrane of Torpedo (16), in the spermatozoan tail (11), and in the inner segment of photoreceptor cells of retina as well as in rod outer segments of photoreceptor cells (12).[2]

Mi-CK mainly associated with the exterior surface of the inner mitochondrial membrane (17, 18) and also found clustered at those peripheral sites where inner and outer mitochondrial membranes are in close vicinity as shown recently by direct ultrastructural immunogold labeling (1) is a key enzyme in oxidative energy metabolism of tissues with sudden high energy demand (for review see Refs. 15, 19–22). It appears to be functionally coupled to the ATP/ADP-translocator (23–26) and is thought to communicate with those CK

* This work was supported by SNF Grants 3.376-086 (to T. W. and H. M. E.) and 3.251-082 (to A. E.) and an ETH graduate training program (to T. S.). The costs of publication of this article were defrayed in part by the payment of page charges. This article must therefore be hereby marked "*advertisement*" in accordance with 18 U.S.C. Section 1734 solely to indicate this fact.

‖ To whom correspondence should be addressed.

[1] The abbreviations used are: Mi-CK and (Mi)-CK refer to the mitochondrial CK isoenzyme and the subunit of Mi-CK, respectively; UC, ultracentrifugation; STEM, scanning transmission electron microscopy; Gdn-HCl, guanidine hydrochloride; EGTA, [ethylenebis(oxyethylenenitrilo)]tetraacetic acid; TMV, tobacco mosaic virus; CP, phosphocreatine.

[2] A. Quest, W. Hemmer, A. Capt, and T. Wallimann, unpublished results.

isoforms that are strategically located at intracellular sites of high energy demand via a creatine-phosphocreatine circuit or shuttle system (21, 27) (for review see Ref. 15).

The results of the structural characterization of Mi-CK by analytical ultracentrifugation (UC), by direct mass measurements with the scanning transmission electron microscope (STEM) and by digital image processing of conventional bright field electron micrographs of either negatively stained or heavy metal-shadowed single octameric Mi-CK molecules presented in this work are fully consistent with the biochemical data obtained (1). Evidence is provided that native Mi-CK can form ordered octameric structures with a molecular mass of 340 ± 55 kDa (by STEM) that consist of four Mi-CK dimers with two identical (Mi)-CK subunits of 43 kDa each. The perforated cube-like structure of the Mi-CK octamer with its central cavity is compatible with the physiological function of the enzyme, that is channeling of high energy phosphate out of the mitochondria. Mi-CK octamers are functionally and perhaps also physically coupled to ATP/ADP-translocators of the inner mitochondrial membrane in a nonstationary, dynamic way. Parts of this work have been presented in abstract form (28, 29).

MATERIALS AND METHODS

Ultracentrifugation—A Beckman model E analytical ultracentrifuge, equipped with ultraviolet absorption optics, a photoelectric scanner, and a Schlieren optical system were used for sedimentation velocity and equilibrium studies. Sedimentation velocity runs were carried out at 20–25 °C with Mi-CK concentrations corresponding to 0.2–0.8 OD absorption at 280–290 nm with An-D and An-E rotors at 56,000 and 52,000 rpm using the 12- and 30-mm double sector Epon cells, respectively. For studies involving urea and Gdn-HCl, Kel-F and Epon-filled charcoal center pieces were used. Absorption scans and Schlieren photographs taken at different intervals during sedimentation velocity runs were used to calculate the sedimentation coefficients.

In order to study the octameric, the dimeric, and monomeric species of Mi-CK, the sedimentation behavior of the enzyme was investigated under native conditions, conditions favoring dimer formation or with increasing concentrations of urea or Gdn-HCl. Values of the actual sedimentation coefficients (s_{obs}) were converted to a standard ($s_{20,w}$, referring to a value of a solution with the density of water at 20 °C). The partial specific volume ($\bar{\nu}$ = 0.73 ml/g) was evaluated from the amino acid composition of Mi-CK derived from cloned chicken Mi-CK cDNA (7) and corresponded to that calculated from canine myocardium (30). For sedimentation equilibrium runs the low speed method was applied after starting with a short overspeed period (31) at protein concentrations of 0.2 and 0.6 OD_{290} nm and absorption scans were recorded after 16–24 h at 20 °C. For molecular mass determinations the best linear fit of ln A *versus* r^2 was computed by using a linear regression computer program (written by H. Berger and A. Lustig, Biocenter for Apple II with graphic pad).

Mass Measurements by STEM—Homogeneous, 3–5 nm thick carbon films were deposited on holey plastic-film-covered 200 mesh EM grids as described (32). After glow discharging immediately before use, the grids were floated for 30 s on drops containing purified Mi-CK diluted to 5–10 μg/ml with storage buffer (5 mM $MgCl_2$, 0.2 mM EGTA, 1 mM β-mercaptoethanol, 50 mM phosphate, pH 8.0). Mi-CK molecules, either fixed for 30 s by transferring the grids onto a drop of 0.05% glutaraldehyde in storage buffer, or unfixed, were placed for 30 s onto a drop of solution containing tobacco mosaic virus (TMV). After washing in four drops of distilled water and blotting off excess liquid, specimens were plunged into liquid nitrogen, mounted in precooled specimen cartridges, and introduced into a STEM (Vacuum Generators, HB-5). The vitrified samples were freeze-dried at −80 °C at 10^{-8} mbar and studied at 80 kV and an irradiation dose of 300–600 $\bar{e}/nm^2$. Under these low-dose conditions damage to molecules resulting in mass loss was negligible (32). Darkfield detector signals of elastically scattered electrons were recorded at a magnification of ×200,000 and stored on disc as images of 512 × 512 pixels, each accommodating 0–255 single electron counts corresponding to 256 gray levels. A UNIVAC-VARIAN V-77-800 minicomputer with a real-time, on-line data aquisition system (VORTEX) allowing for digital gray-level integration was used for mass measurements (34). The mass/length values of TMV particles and the mass of Mi-CK dimers and octamers were evaluated from dark field images as described (32, 33). To calibrate the system for absolute mass determination the theoretical value for TMV (131.5 kDa/nm) (35) was used as standard (32), yielding normalization factors that were close to unity (±10%) throughout the experiments.

The mass of visually selected Mi-CK particles was computed by using the INTARE program (34) which determines the mass of macromolecules within a circular area after correction for empty carbon film background. In parallel, the INTBOX program which determines first the contour of a selected particle and then the mass within this contour was also applied. The contour threshold was chosen to minimize inclusion of background material but without cutting off significant contribution due to molecular mass of Mi-CK molecules in order to reduce statistical noise (33). Mass increase due to bound glutaraldehyde was found to be approximately 10% of the total mass[3] and was corrected for accordingly (Table I). Histograms of mass data were generated, their mean values and standard deviations computed, and the distribution fitted by Gaussian curves with a Marquardt algorithm (36).

Electron Microscopy—Carbon-coated glow-discharged 400 mesh copper electron microscope grids were placed for 1 min on a drop of Mi-CK solution at 10–20 μg/ml in storage buffer (5 mM $MgCl_2$, 0.2 mM EGTA, 1 mM β-mercaptoethanol, 50 mM sodium phosphate at pH 7.0–8.0). Liquid was blotted off, the specimens washed in buffer and quartz-distilled water, and finally stained for 15 s in 2% aqueous uranyl acetate, pH 4.3. For freeze-drying and heavy metal-shadowing experiments, droplets of freshly diluted Mi-CK were deposited onto glow-discharged carbon grids, washed as above, but subsequently inserted on a magnetic table that was plunged into liquid nitrogen. The table was introduced onto a precooled stage (Balzers BAF 300) at −80 °C and freeze-dried for 30 min at −35 °C at $p \leq 10^{-6}$ mb. Rotary shadowing (at 80 rpm) was done at 15°, 30°, and 45° elevation with 10–15 Å of Pt/C followed by backing with 100 Å of carbon. Pictures were taken with a Jeol JEM 100C or a Philips 300 electron microscope equipped with liquid nitrogen anticontamination devices. Images were recorded at a nominal magnification of × 50,000 on Agfa-Gevaert Scientia film or Kodalith LR 70 mm roll film. To reduce beam damage pictures of negatively stained molecules were obtained by blind shots. Catalase crystals were used for calibration of magnification. Optical diffraction was used to select images with corrected astigmatism and optimal focus (37).

Image Processing of Single Particles—Areas of electron microscope negatives suitable for image processing were scanned by an Optronics P-1000 drum-type microdensitometer at a sampling raster of 50 μm forming images of 512 × 512 pixels. Data were stored on tape and processed by the SEMPER image processing system (38). Galleries of particles visually selected by their structural preservation and clarity of details were generated. Single particles were then aligned angularly and translationally by correlation techniques with respect to a reference motive built up from three well-preserved, intact molecules. Cross-correlation of the reference particles with the aligned single molecules served to select molecules with more than 75% similarity to the reference that were finally averaged and subjected to 4-fold symmetrization. Processed pictures were displayed by a monitor and recorded an Ilford HP5 film.

RESULTS

Molecular Weight, Oligomeric Structure, Shape, and Stability of Mi-CK—Sedimentation velocity analysis under native conditions of either fresh Mi-CK directly purified from cardiac mitochondria or after prolonged storage (for months) at concentrations of ≥1 mg/ml in liquid N_2 revealed sharp absorption boundaries and symmetrical Schlieren peaks (not shown), corresponding to a homogeneous population of molecules. The calculated sedimentation coefficients of 12.8 and 13.5 S, using Schlieren optics and absorption techniques, respectively, indicate a high molecular weight species for Mi-CK (Table I). The M_r was determined by sedimentation equilibrium runs to be 321,000 and 328,000 ± 25,000 at protein concentrations of 0.6 and 0.2 mg/ml, respectively (Table I). These values correspond to an octameric (Mi-CK species with

[3] A. Engel, unpublished results.

TABLE I

Mean values for the molecular mass of Mi-CK octamers, dimers, and monomers by analytical ultracentrifugation and direct mass measurements by STEM

Sedimentation coefficient $s_{20,w}$ for Mi-CK octamers, dimers, and monomers determined by using absorption scan techniques[b] and Schlieren optics[a] under native conditions (5 mM $MgCl_2$, 0.2 mM EGTA, 1 mM β-mercaptoethanol, 1 mM NaN_3 in 50 mM sodium phosphate buffer at pH 8.0), in the presence of Mg-ADP, creatine, and nitrate to induce dimer formation, or in the presence of 6 M guanidine HCl to form monomers. Molecular weight (M_r) as determined by sedimentation equilibrium runs under native conditions (protein concentration for octamers at 0.6 mg/ml[c] and 0.2 mg/ml[d] and for dimer at 0.5 mg/ml) as well as in 6 M guanidine HCl to give monomers. Direct mass measurements by STEM of glutaraldehyde-fixed and unfixed Mi-CK octamers and dimers under native conditions. Values[d] include mass of bound glutaraldehyde which is corrected for accordingly in[e] as described under "Materials and Methods."

	By analytical UC		
	Mi-CK octamer	Mi-CK dimer	Mi-CK monomer
$S_{20,w}$	12.8[a]–13.5[b]	~5.0	2.0[b]
M_r	321,000[c]–328,000[d] ±25,000	83,000 ±8,000	45,000 ±4,000

	By STEM	
	by INTARE program	by INTBOX program
	kDa	
Mi-CK octamer fixed[d]	378 ± 60	340 ± 49
Mi-CK octamer fixed[e]	340 ± 55	
Mi-CK octamer unfixed	328 ± 70	
Mi-CK dimer fixed[d]	106 ± 32	89 ± 27
Mi-CK dimer fixed[e]	95 ± 30	

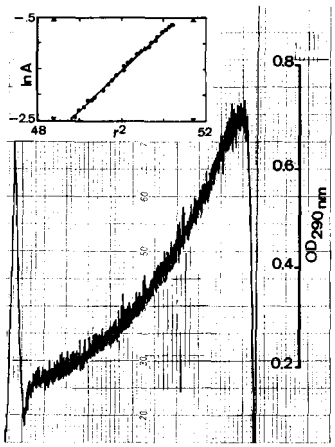

FIG. 1. **Sedimentation equilibrium analysis of Mi-CK octamers by analytical ultracentrifugation under native condition at 20 °C running temperature and 6,400 rpm rotor speed showing an actual absorbance tracing (OD at 290 nm) and a computed data set where ln A is plotted against r^2.** Number of data read = 30, base line = 0.113 OD, slope = 0.776, linear correlation factor = 0.9998, and of the molecular weight of Mi-CK octamers determined to be 320,475 ± 5%.

8 subunits of 42,000 each (determined by sodium dodecyl sulfate-polyacrylamide gel electrophoresis) or of 43,195 kDa each (by molecular cloning of Mi-CK cDNA, Ref. 7), the latter two amounting to M_r values of 336,000 or 345,560 for a Mi-CK octamer. The molecular homogeneity of Mi-CK indicated by absorption scans of the sedimenting protein preparation and the resulting linearity of ln A *versus* r^2 are shown in Fig. 1. The data are in good agreement with those obtained by gel permeation (364,000 ± 30,000, Ref. 1) and with the direct mass measurements by STEM (340,000 ± 55,000, Table I, see above). Thus, by all criteria it is safe to assume that Mi-CK forms homogeneous octameric structures.

The dry volume (hydration number $\delta = 0$) of the Mi-CK octamer calculated from the M_r of 328,000 and the partial specific volume of chicken cardiac Mi-CK ($\bar{\nu} = 0.730$) was 400 nm^3. The resulting frictional ratio f/f_0 of 1.25 (f is the experimentally determined and f_0 the calculated frictional coefficient of a sphere of 400 nm^3) allows for a maximal assymetry with an axial ratio (a/b) of 6.5. According to Tanford (76) this value is still compatible with a globular protein. On the other hand, a maximal volume of 800 nm^3 corresponding to a fully hydrated octamer with a frictional ratio f/f_0 of 1 is obtained by a hydration number $\delta = 0.72$ g of H_2O/g of protein. This volume for the hydrated Mi-CK octamer is in good agreement with the dimensions of the cube-like molecules (1000 nm^3) with a side length of 10 nm each estimated by electron microscopy.

Hydrodynamic measurements are consistent with the theoretical s value obtained by modeling of a structure composed of four cylinders in a cubic arrangement according to the theory of Bloomfeld *et al.* (39). Such a model is supported by direct visualization of single Mi-CK octamers in the electron microscope where molecules of 4-fold symmetry consisting of four domains that each correspond to one of the Mi-CK dimers are demonstrated (Figs. 3 and 4).

Ultracentrifugation analysis of Mi-CK from bovine heart (40)[4] demonstrated the stability of Mi-CK octamers in a variety of buffers within a pH range of pH 6.5–8.0 and within a wide range of salt conditions including physiological ionic strength that seem to have a stabilizing effect on the octamer (1). Thus, the formation of octamers was not dependent on the buffers used during our isolation procedure and for storage. These data are in agreement with those obtained by gel permeation chromatography and electron microscopy (see Table I).

Sedimentation equilibrium runs in the presence of increasing amounts of urea and Gdn-HCl revealed that small concentrations of denaturing agents were sufficient for destabilization of the octameric structure and lead to complete conversion of octamers into dimers. However, the dimers generated were of remarkable structural stability. The experimental s value of 5 S for the Mi-CK dimer obtained by forming transition-state dead-end complexes is similar to that determined for cytosolic Mi-CK (77), which was found to be cigar-shaped (77). Mi-CK dimers did withstand 1–2 M urea and only completely dissociated into monomers with an s value of 2.0 S in the presence of 6 M Gdn-HCl.

Direct Mass Measurements by STEM—Unstained, "naked" Mi-CK molecules were visualized by STEM (Fig. 2, *a* and *b*). Two different kinds of particles could be discerned, larger roundish or square-type, and a few smaller elongated ones, corresponding to Mi-CK octamers and Mi-CK dimers, respectively. Glutaraldehyde-fixed particles were preserved somewhat better and, although no specific submolecular details were resolved, fixed Mi-CK particles appeared to exhibit a 4-fold symmetry. More than 900 subframes (containing Mi-CK particles and empty carbon film) were processed using the INTARE program (34) to generate the mass distribution profiles depicted in Fig. 2*c*. Two sharply peaked maxima were resolved at 1579 and 1201 kDa corresponding to the mass distribution of Mi-CK octamers plus carbon support and carbon film alone, respectively. The averaged difference in mass due to Mi-CK protein itself was therefore 378 ± 60 kDa for the glutaraldehyde-fixed octamer (Table I). Subtraction

[4] T. Schnyder, A. Engel, A. Lustig, T. Wallimann, unpublished observations.

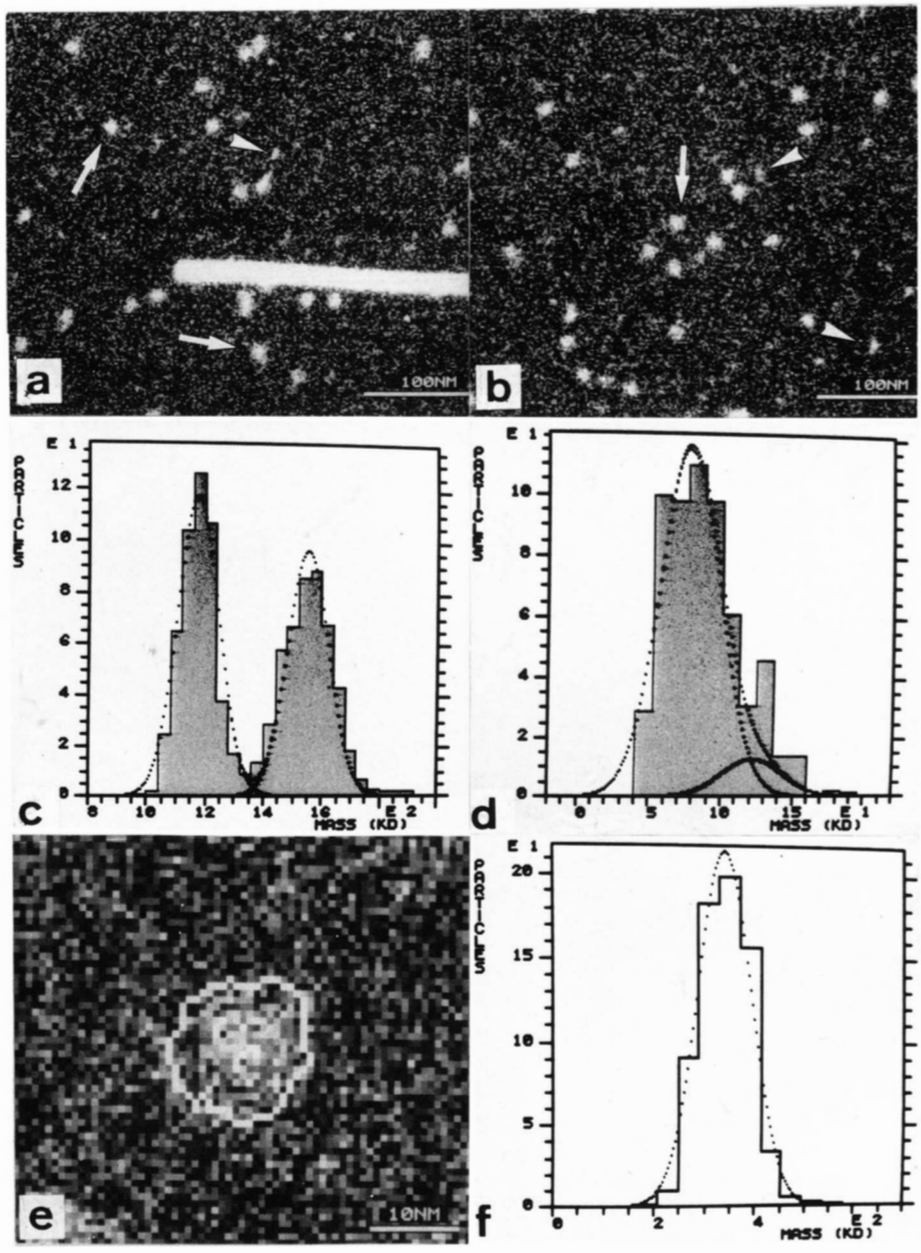

FIG. 2. **Direct mass measurements of Mi-CK molecules by STEM.** Glutaraldehyde-fixed unstained Mi-CK molecules visualized by STEM together with tobacco mosaic virus (TMV) used as a molecular mass standard. *Large arrows* point out Mi-CK octamers, *small arrowheads* indicate Mi-CK dimers in two fields (*a* and *b*, *bars* = 100 nm). Mass distribution of more than 900 subframes containing Mi-CK octamers plus the underlying carbon film (Gaussian peak at 1579 kDa) and of carbon film background alone (peak at 1201 kDa) evaluated by the INTARE program, yielding a molecular mass of 378 ± 60 kDa for glutaraldehyde-fixed Mi-CK octamers (*c*). Mass distribution of 600 subframes containing fixed Mi-CK dimers as determined by INTBOX program by which the mass within the contoured area around the particles was directly calculated as being 89 ± 27 kDA (*d*, note: histogram was fitted best by two Gaussians with a large peak at 78 kDa with a half-height width of 21 kDa). Example of a glutaraldehyde-fixed Mi-CK octamer particle contoured by the INTBOX program (*e*, *bar* = 10 nm), and the corresponding mass distribution for a total of 680 subframes octamers processed by this method revealing a peak at 340 ± 49 kDa (*f*).

of 10% mass due to bound fixative resulted in a final mass of 340 ± 55 kDa. The same evaluation program, applied to approximately 600 subframes with unfixed octamers, revealed a mass of 328 ± 70 kDa (data distribution not shown). The larger standard deviation of unfixed compared with fixed octamers, however, suggests some dissociation of octamers during washing, thus justifying a global correction factor of 0.9 for fixed particles. A similar value of 340 ± 49 kDa was obtained by averaging 700 subframes of fixed molecules using the contour setting program INTBOX (33). A contoured octamer is shown in Fig. 2*e*, and the respective histogram of mass distribution fitted by Gaussian profile is illustrated in Fig. 2*f*. For the mass determination of dimeric Mi-CK, only fixed preparations were investigated as they showed a significantly better signal-to-noise ratio which is critical if molecules of such low mass are measured. Analysis of 600 subframes contoured by the INTBOX programm gave an average of 89 ± 27 kDa for Mi-CK dimers (Fig. 2*d* and Table I). The same set of Mi-CK dimers was subjected to the INTARE computer program to give 106 ± 32 kDa. The value is reduced to 95 ± 30 kDa assuming a 10% mass contribution due to fixative.

The M_r numbers obtained by direct mass measurements of Mi-CK molecules in the STEM are in excellent agreement with hydrodynamic data (see Table I) and confirm (*a*) the existence of Mi-CK octamers as well as dimers and (*b*) support the notion that Mi-CK exists as two interconvertible forms, which also was shown by biochemical means in the preceding publication (1).

Electron Microscopy of Mi-CK and Single Particle Averaging—Fields of randomly distributed single molecules adsorbed onto glow-discharged carbon films shown after negative staining (Fig. 3*a*) clearly revealed a homogeneous population of square-shaped molecules with a side length of about 10 nm each and a central negative stain-filled cavity or channel of 2.5–3 nm in diameter (Fig. 3*a*). Molecules that were rotary-shadowed with heavy metal exhibited a central indentation of similar dimensions which often suggested a "cross-like" surface (Fig. 3*b*). The octamers showed 4-fold symmetry, and the four identical subunits seen in Fig. 3 correspond most

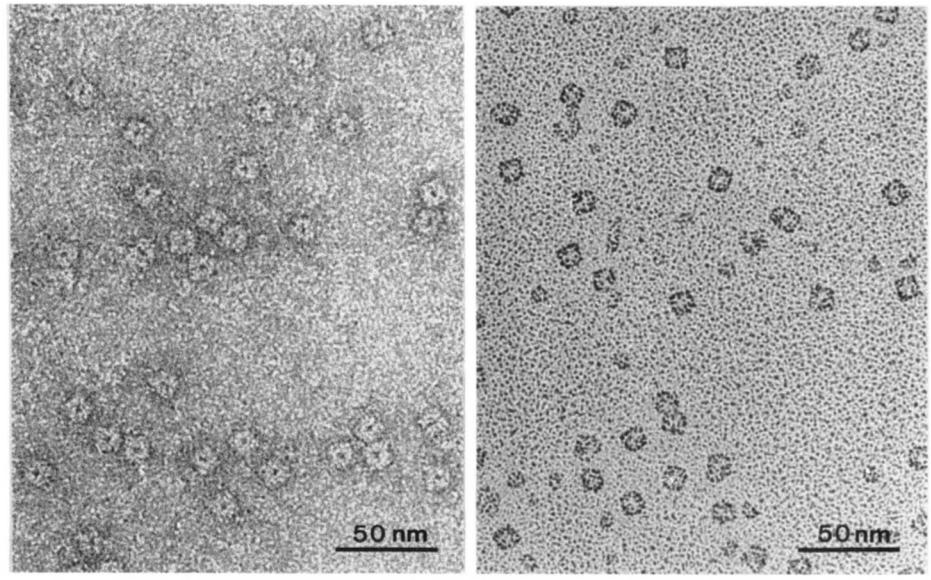

FIG. 3. **Negatively stained and rotary-shadowed Mi-CK molecules by conventional transmission electron microscopy.** Conventional transmission electron micrographs of a field of Mi-CK molecules negatively stained with uranyl acetate showing almost exclusively Mi-CK octamers with 4-fold symmetry and a central cavity or channel that is filled by negative stain (*a, bar* = 50 nm). Field of Mi-CK molecules rotary shadowed at an angle of 30° with Pt/C, also showing mostly Mi-CK octamers with a central indentation (*b, bar* = 50 nm).

likely to four Mi-CK dimers which are arranged around a central cavity to form the octamer. These features became more distinct after image processing, when galleries of subjectively chosen Mi-CK molecules, either negatively stained or rotary shadowed, (Fig. 4, *A* and *B*) were aligned with respect to a reference motif and averaged (*a1* and *b1*), and were either displayed as contour maps (*a3* and *b3*) or in gray-level display (*a4* and *b4*). Among the negatively stained averaged molecules (*a4*), the 4-fold symmetry is reinforced by the pointed corners giving rise to a windmill-like molecule (protein = white) with a central hole filled with negative stain. On the other hand the averaged molecules, rotary shadowed by heavy metal (*b4*) exhibited more rounded corners, giving rise to cube-like particles (protein = dark), but also showed the central indentation. In addition to the central hole seen as a prominent feature of negatively stained molecules, the surface relief of shadowed molecules revealed a radial cross-like conformation (*b2* and *b4*) as also indicated in the schematic model of the Mi-CK octamer (Fig. 5). Unidirectional heavy metal shadowing of octamers at 45° and measurements of shadow lengths revealed that the height of Mi-CK octamers was similar to the side lengths (10 nm). This points to a cube-like oligomeric structure of the Mi-CK octamer as pictured schematically in Fig. 5. The dimensions of Mi-CK dimers (banana-shaped cylindrical structures seen in Fig. 2*b*, *arrowheads*, and Fig. 6 from Ref. 1) were also approximately 10 nm in length and some 6–7 nm in diameter. Thus, the length of a dimer corresponded to the height of an octamer, and the diameter of a dimer was approximately half that of an octamer. These data are consistent with the model that four Mi-CK dimers arranged around a central pit or trans-channel form a cube-like Mi-CK octamer. Such a structure for octameric Mi-CK is favored also by ultracentrifugation studies and theoretical modeling of hydrodynamic parameters that provide best fits for a cubic arrangement of four identical cylinders, presumably represented by the four Mi-CK dimers (39).

DISCUSSION

Oligomeric State and Shape of Cardiac Mi-CK—The results presented in this work together with the biochemical characterization of Mi-CK shown in the preceding publication (1) provide unequivocal evidence for the existence of native Mi-CK in a defined oligomeric state, that is an octamer exhibiting a regular cube-like structure with 4-fold symmetry and a central cavity. Analytical ultracentrifugation studies confirmed the purity of cardiac Mi-CK and the presence within these preparations of homogeneous populations of octamers and dimers varying in proportion as a function of experimental conditions (the presence of adenine nucleotides and dilution of the protein to low concentrations leading to fast and slow formation of dimers from octamers, respectively (1). However, fresh cardiac Mi-CK, purified according to the procedures described (1), contained ≥95% of the octameric species. In contrast to earlier reports (41) no higher M_r aggregates and no long-lived stable intermediates between octamers and dimers, *e.g.* hexamers and tetramers were found by analytical UC indicating a rapid dimer-octamer equilibrium and a high cooperativity between dimers to form octamers. These findings are fully supported by gel permeation chromatography on fast protein liquid chromatography Superose-12 columns and indicate that upon concentration of a Mi-CK dimer solution, previously obtained on a slow time scale (within days) by dilution of an octamer solution to lower than 0.2–0.5 mg/ml, the reconversion of dimers to octamers is a very fast (within minutes) and highly cooperative process (1). The remarkable stability of Mi-CK dimers toward denaturing agents (withstanding 1–2 M urea) observed by analytical UC studies was also confirmed by sodium dodecyl sulfate-polyacrylamide gel electrophoresis and immunoblotting of purified Mi-CK where often a faint protein band corresponding in apparent M_r to the Mi-CK dimer position was observed. This minor band varying in intensity did react with polyclonal as well as with monoclonal anti-Mi-CK antibodies. Characterization of the Mi-CK octamer by UC indicated a rather compact globular particle with a sedimentation coefficient of 12.8–13.5 S, that was best-fitted theoretically according to Bloomfield *et al.* (39) by a model consisting of four equal cylinders to form a cube-like structure (with theoretically calculated *s* values of 13.8 and 12.7 S at 0 and 20% hydration, respectively). A cube-like molecule consisting of four equal Mi-CK dimers (cylinders), of course, is in excellent agreement with the actual shape of Mi-CK octamers and with the 4-fold symmetry revealed by electron microscopy.

Mass Measurements by STEM—At first glance the mass measurement data obtained by STEM show somewhat larger standard deviations than results obtained by UC, but the average mass values obtained by STEM are in better agreement with recent sequence data (7), and the histograms

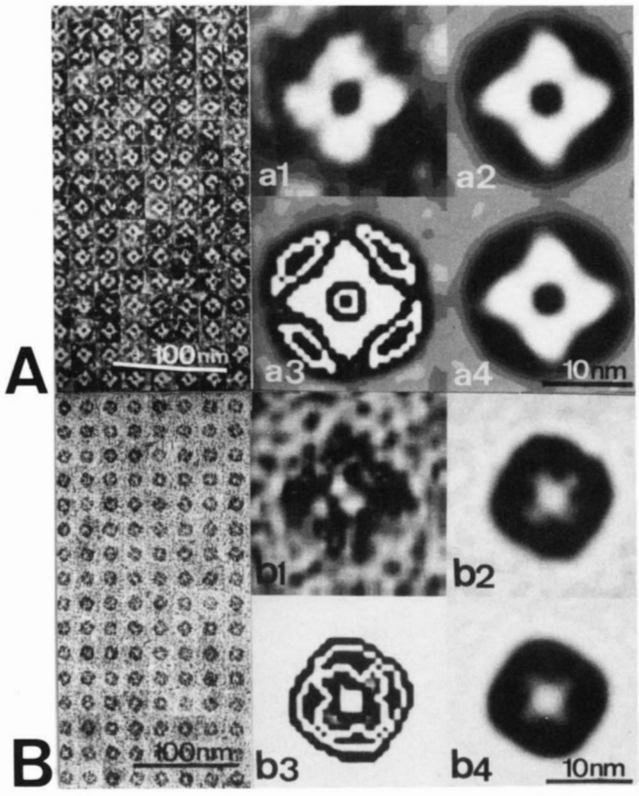

FIG. 4. **Structure of Mi-CK octamers after image processing of negatively stained and rotary-shadowed single molecules visualized by conventional transmission electron microscopy.** Conventional transmission electron microscopy of Mi-CK octamers after negative staining with uranyl acetate (gallery of 192 molecules in *A*, *bar* = 100 nm); and rotary shadowing with heavy metal under standard conditions (gallery of 192 molecules in *b*, *bar* = 100 nm). Molecules selected by eye are displayed in the two galleries (*A* and *B*) after two cycles of angular and linear alignment by computer (SEMPER image processing program) using the enlarged reference motifs (*a1* and *b1*), an averaged structure of the three best molecules subjectively selected as reference motifs. Gray-level display of processed images of the average structures after addition of 167 images of negatively stained (*a2*) and 127 images of rotary-shadowed particles (*b2*), respectively, showing more than 75% similarity to the reference motif by cross-correlation. The same average structures in contour representation (*a3, b3*) and finally the 4-fold symmetrized and averaged structures (4 × 167 negatively stained molecules in *a4*; and 4 × 127 shadowed molecules in *b4*) are shown in gray-level display. Molecular mass appears white in negatively stained, windmill-like structures and black in rotary-shadowed, square-shaped structures, respectively. *Bars* in *A* and *B* are 100 nm; *bars* in *a1* to *b4* are 10 nm.

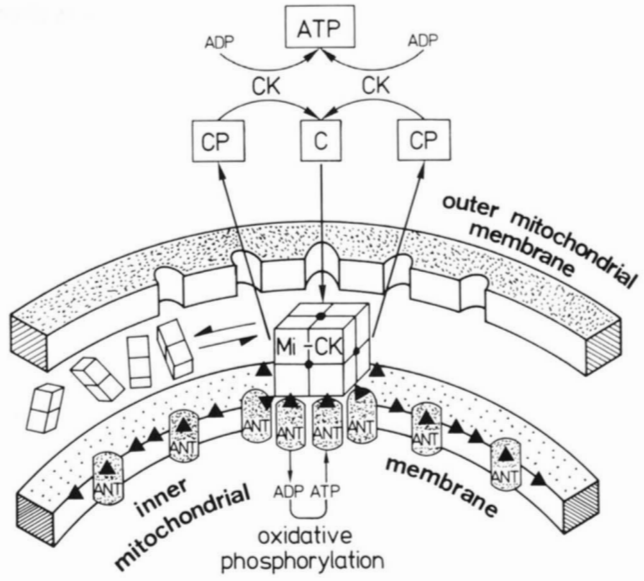

FIG. 5. **Model of mitochondrial CK function in energy transport.** 1) The octameric nature of Mi-CK and its association with four or eight cardiolipin-coated (▲) ATP/ADP-translocator dimers (*ANT*), 2) the temporarily compartmented and functional coupling of the two molecules, and 3) the existence of separate, relatively small ATP/ADP pools with rapid turnover are depicted here. The model tries to show *a*, the postulated dynamics of the octamer-dimer equilibrium within the intermembrane space regulated, *e.g.* by adenine nucleotides (see Ref. 1), *b*, the reversible, preferential interaction of Mi-CK octamers with the inner mitochondrial membrane, and their postulated cyclic association with translocator-dimers (*ANT*), and *c*, the probable involvement of the outer mitochondrial membrane in the compartmented, functional coupling by forming outer-inner membrane contact sites that have been shown to be enriched in translocase, Mi-CK, and hexokinase activity (59, 75). The structure-function relationship of Mi-CK octamer as a candidate for channeling of high energy phosphate in the form of CP is indicated stressing the mitochondrial side of the CP shuttle. According to this model the high energy phosphate leaving the mitochondria of tissues with high, sudden energy requirements (muscle, brain, photoreceptor cells, spermatozoa etc.) is phosphocreatine (*CP*), and not ATP, the latter being generated by creatine-, ADP-, and P_i-stimulated oxidative phosphorylation. CP produced by this way is fed into a large cytoplasmic CP pool and is made available from there to sites of high ATP demand where compartmented "cytosolic" CK isoforms (*CK*) are specifically located to control local ATP levels (for review see Ref. 15).

exhibit convincing Gaussian peaks (Fig. 2). The fact that relative data scattering was larger with particles of lower mass (compare Mi-CK dimers with Mi-CK octamers) simply reflects a lower signal-to-noise ratio due to local variations in background and possible small contaminations on the support films. However, since the error of the mean mass value is equal to the standard deviation divided by the square root of the number of particles measured, it was demonstrated here that with as many as 300–600 particles measured the accuracy of the mean mass value is within 3 and 8% for the octamers and dimers, respectively. The fact that both mean values are in remarkably close agreement with the hydrodynamic data from analytical ultracentrifugation (compare Table I), with the gel permeation chromatography measurements (Figs. 4 and 5 of preceding paper) and with recent sequence data of Mi-CK (7) validates the STEM method. These measurements represent independent additional support for the existence of defined Mi-CK octamers by direct measurements of the actual physical mass of Mi-CK based on electron scattering. No indication in the existence of intermediate forms, *e.g.* tetramers or hexamers was found by STEM either. This result, as well as those obtained by UC, indicate a direct octamer-dimer equilibrium without long-lived intermediates.

It is interesting to note that the corrected mean mass value for fixed Mi-CK particles (340 kDa) was somewhat higher than that of unfixed octamers (328 kDa) indicating that the integrity of the octamers was stabilized, and dissociation into dimers due to factors like dilution of the protein was prevented by chemical fixation. This fact may be especially helpful for the future when more labile complexes are to be studied, *e.g.* the brain-type Mi-CK isoform isolated recently also forms octamers, but they are significantly less stable than cardiac-type Mi-CK octamers (42, 43). Thus, it is of significant importance to have a correction factor of 0.9 established for correction of the glutaraldehyde contribution in fixed oligomers.

Electron Microscopy—Negatively stained Mi-CK octamers were uniform structures with 4-fold symmetry and a central region filled by negative stain that may be interpreted as (*a*)

a more or less water filled inner space or cavity, (*b*) a superficial pit, or (*c*) a transverse channel with openings at both ends. Since rotary shadowing revealed a central indentation in the surface relief it is likely that connections of the central cavity to the surface(s) of the cube-like molecule exists. Assuming that Mi-CK is indeed an energy-channeling molecule (Fig. 5), the concept of an octameric molecule with a central channel could suggest an attractive structure-function relationship. The diameter of the central negative stain seen in the projection is approximately 2.5 nm, but, like other channels, this may vary as a function of physiological states. The fact that we were not able to distinguish different side views of the same octamer molecules indicates that (*a*) the molecule may preferentially adsorb to the glow-discharged carbon film by the two identical "channel-sides" (top and bottom of the cube-like octamer in Fig. 5) or (*b*) that all six sides of the cube-like molecule are very similar or identical. If four dimers with two catalytic sites each are arranged by 4-fold symmetry around a central cavity or channel, it becomes very tempting to speculate that the total of eight catalytic sites (one/subunit) are all directed toward the central opening, thus providing the biochemical and physical basis for a cooperative multisubunit channel protein.

The model that we propose for the Mi-CK octamer is pictured schematically in Fig. 5 where the octamer is drawn as a cube-like molecule with a central main-channel perpendicular to the plane of inner and outer membrane attachments allowing the flux of high energy phosphate (CP). Image reconstruction of negatively stained as well as rotary shadowed molecules indicated also radial cross-like indentations in the relief that originate from the central hole and extend to the periphery (Fig. 4, *b2* and *b4*). This again clearly reinforces the 4-fold symmetry. Such an interpretation is consistent with recent results obtained by high resolution shadowing where cross-like indentations on top of the molecules were clearly resolved (78). The different appearance of contours around Mi-CK octamers after negative staining (pointed corners giving windmill-like appearance) and rotary shadowing (roundish corners) may arise from the fact that the negatively stained molecules were air-dried at room temperature and showed a tendency to disintegrate radially into the four subdomain dimers. For rotary shadowing, however, the molecules were quickly frozen and freeze-dried at low temperature, thereby presumably better preserving the integrity of the oligomeric structure. Therefore, the compact cube-like structures with rounded corners seen in Fig. 4*b* and as a model in Fig. 5 are more likely to correspond to the real shape of the Mi-CK octamer. This is corroborated by negative staining of Mi-CK crystals recently obtained in our laboratory (78).

Functional Coupling between Mitochondrial CK and ATP/ADP-translocator—The concept of functional coupling between Mi-CK and ATP/ADP-translocase in cardiac mitochondria was initially developed on the basis of biochemical and kinetic evidence using isolated mitochondria (24, 44, for review see Ref. 20). This concept as well as a more general CP shuttle hypothesis recently gained support from ^{31}P NMR saturation transfer experiments in normal and ischemic perfused hearts (45–51) where evidence had been provided by NMR for compartmentation of the CP/CK system in combination with the existence of distinct adenine nucleotide pools. Similar results had also been obtained by using other methods, like CP depletion and O_2 uptake measurements (52–54, 70) or biochemical (71) and physiological (72, 73) approaches. In addition, the existence of mitochondrial adenine nucleotides that are "invisible" to ^{31}P NMR due to binding has been discussed (48, 50, 55). Furthermore, recent experiments (56) indicated that antibodies against Mi-CK not only blocked Mi-CK activity, but also oxidative phosphorylation of extramitochondrially added ADP, presumably by sterically inhibiting ATP/ADP-translocator activity as well. A close spatial proximity between Mi-CK and translocase is supported by these data. Although Mi-CK was thought earlier to be exclusively located on the inner mitochondrial membrane, an involvement of the outer mitochondrial membrane in a compartmented functional coupling between Mi-CK and translocators (*ANT*, Fig. 5) has now become apparent (57, 58). The outer mitochondrial membrane is thought to stabilize an unstirred layer existing between inner and outer mitochondrial membrane apparently by creating a partial diffusion barrier to charged molecules like ADP, ATP, and CP but not to creatine governed by voltage-gated pores (74, 75). This would result in an increased concentration of adenine nucleotides in the intermembrane space *versus* the bulk concentration in the cytosol and hence would cause compartmented coupling (58) by affecting both Mi-CK and ATP/ADP-translocator enzyme kinetics. However, additional new factors worth consideration may play a crucial role in increasing the efficiency of mitochondrial energy transport, *e.g.* the formation of clustered Mi-CK-translocator complexes between the outer and inner mitochondrial membranes that transitorily connect the peripheral inner mitochondrial matrix via translocator and Mi-CK channels and via outer membrane pores to the cytoplasm. Such channeling complexes are likely to regulate and increase the efficiency of creatine uptake and ATP and CP extrusion of mitochondria (see Fig. 5). In accordance with this, Mi-CK was found by direct ultrastructural immunolocalization to reside not only along the inner mitochondrial membrane, but was also shown to be clustered at those peripheral regions where inner and outer mitochondrial membranes were in close vicinity (1). In addition, Mi-CK was enriched in isolated boundary membrane contact site preparations (59, 75). Furthermore, Mi-CK exists in two interconvertible forms, octamer and dimer, whereby the octamer-dimer equilibrium is affected by adenine nucleotides and additional factors as well (1). Finally, the higher M_r form of Mi-CK, described by Marcillat *et al.* (60), presumably corresponding to the octamer characterized herein, did rebind preferentially over the dimer to the mitochondrial inner membranes of mitoplasts (60).[5] All these findings support the above hypothesis.

The role of cardiolipin, a prominent, highly negatively charged phospholipid of the inner mitochondrial membranes which had been purported as *the* receptor for Mi-CK (61) remains rather unclear, for the Mi-CK/cardiolipin interaction is strongest at very low salt concentration, but decreased to less than 20% at physiological ionic strength (Fig. 3 of Ref. 61). In addition, some totally unrelated nonmitochondrial proteins, *e.g.* the complement factor Clq in the blood also bind to cardiolipin with comparable affinity (62). Since all these proteins have an extremely high isoelectric point (chicken cardiac Mi-CK = pH 9.3–9.5) and cardiolipin is negatively charged under physiological conditions, an artifactual association cannot be excluded. Furthermore, the argument that an interaction between Mi-CK and ATP/ADP-translocator is impossible due to the overall basic nature of both proteins involved (61) may not apply to local surface domains of the two proteins which still could favor an interaction between the two. NMR data have revealed that isolated ATP/ADP-translocator retains a total of six tightly bound cardiolipin molecules/translocator dimer (63). Thus, together with our new findings on the structure and localization of Mi-CK as well as those on the preferential rebinding of octamers to the

inner mitochondrial membrane (60),[5] it seems reasonable to propose that the interaction of Mi-CK with translocators be a complex and dynamic one. The process would involve a specific interaction of the octamer with the inner mitochondrial membrane via free, or more likely via translocator-bound cardiolipin, as an initial anchor or homing device. This could then mediate a specific protein-protein interaction between Mi-CK octamers and ATP/ADP-translocators to form a transitory multienzyme complex which may be stabilized by interaction with the outer mitochondrial membrane at sites where boundary membrane contact sites are temporarily being formed, *e.g.* during stimulation of oxidative phosphorylation (64). Some of the ideas on the structure and function of Mi-CK in mitochondria within tissues of sudden, high energy requirements are put together in a simplified model (Fig. 5) that is based on experimental findings and provides a conceptual framework for future studies. It is tempting to speculate that the localization and physical interaction of Mi-CK with the ATP/ADP-translocator and with mitochondrial membranes is likely to be dynamic and to depend, for example, on the respiratory state of the mitochondria, since the octamer-dimer equilibrium (1) as well as the binding of Mi-CK to mitochondrial membrane(s) (60) is dependent on adenine nucleotides. The model shown in Fig. 5 depicts parts of the proposed dynamic regulatory circuit.

As judged by the 4-fold symmetry and the relative size of Mi-CK octamers compared to ATP/ADP-translocator dimers, a complex consisting of four or eight translocator dimers/one CK octamer would seem reasonable. Such complexes should *not* be envisaged as permanent ones but rather should reflect an optimal functional unit generated by frequent collision due to lateral diffusion of the molecules on the inner mitochondrial membrane. Since the stoichiometry of Mi-CK to translocator, contrary to what has been reported earlier (65), is by far lower than 1 to 1 (see Ref. 1), obviously, such complexes between one Mi-CK octamer and four or eight translocator dimers can only be of transient nature.

Even though on an absolute scale significantly less Mi-CK than translocase is present in mitochondria, the much higher substrate turnover rate of Mi-CK compared to that of translocase (see Ref. 1) would be more than sufficient to serve all translocators if Mi-CK were to "jump" on the membrane, form complexes, and possibly dissociate off again. Furthermore, binding of Mi-CK to mitochondrial membranes and/or translocator may additionally enhance its turnover rate.

Such transient stoichiometric arrangements together with an involvement of the outer mitochondrial membrane (58, 59) may be mediated by regulatory factors such as substrate (CP/C) and cofactors (ATP/ADP) as well as by pH, Mg^{2+}, and phosphate that all have been shown to affect Mi-CK structure or its association with mitoplasts (Refs. 56, 60, 66–69). Last but not least, a possible voltage-gated regulation of the anion-selective pore of the outer mitochondrial membrane may regulate the flow of metabolites in conjunction with the CK octamer in the contact sites (59), where the pore is proposed to close for anions like ATP, ADP, and CP but to let pass creatine (74, 75 and references therein).

It will be very exciting to test some of these hypotheses and unequivocally identify the physiological factors that favor close functional and structural coupling between Mi-CK octamers, ATP/ADP-translocators, and mitochondrial membranes. The physiological relevance of Mi-CK octamers and dimers calls for crystallization of the two purified forms, for only then can some of the most pressing structural questions on this interesting oligomeric enzyme be answered and a structure-function relationship of the highly ordered Mi-CK octamer be established.

[5] J. Schlegel and T. Wallimann, unpublished results.

Acknowledgments—We thank Drs. H. M. Eppenberger for support, Dr. A. Quest, J. Schlegel, M. Wyss, Drs. H. Gross and M. Klingenberg for discussions, Drs. H. K. Jacobs and D. Brdiczka for communication of unpublished results concerning an analytical ultracentrifugation study with Mi-CK from bovine heart and identification of Mi-CK at isolated contact sites, respectively. Special thanks go to Dr. Rudolf Reichelt, Biocenter, Basel, for his generous help and valuable discussion throughout this work. R. Amatore, E. Abächerli, and M. Leuzinger are acknowledged for typing.

REFERENCES

1. Schlegel, J., Zurbriggen, B., Wegmann, G., Wyss, M., Eppenberger, H. M., and Wallimann, T. (1988) *J. Biol. Chem.* **263,** 16942–16953
2. Jacobs, H., Heldt, H. W., and Klingenberg, M. (1964) *Biochem. Biophys. Res. Commun.* **16,** 516–527
3. Jacobus, W. E., and Lehninger, A. L. (1973) *J. Biol. Chem.* **248,** 4803–4810
4. Eppenberger, H. M., Dawson, D. M., and Kaplan, N. O. (1967) *J. Biol. Chem.* **242,** 204–209
5. Blum, H. E., Weber, B., Deus, B., and Gerok, W. (1983) *J. Biochem. (Tokyo)* **94,** 1247–1257
6. Brooks, S. P. J., Bennett, V. D., and Suelter, C. H. (1987) *Anal. Biochem.* **164,** 190–198
7. Hossle, J. P., Schlegel, J., Wegmann, G., Wyss, M., Böhlen, P., Eppenberger, H. M., Wallimann, T., and Perriard, J. C. (1988) *Biochem. Biophys. Res. Commun.* **151,** 408–476
8. Roberts, R. (1980) in *Heart Creatine Kinase* (Jacobus, W. E., and Ingwall, J. S., ed), pp 31–47, Williams & Wilkins Baltimore
9. Booth, R. F. G., and Clark, J. B. (1978) *Biochem. J.* **170,** 145–151
10. Tombes, R. M., and Shapiro, B. M. (1985) *Cell* **41,** 325–334
11. Wallimann, T., Moser, H., Zurbriggen, B., Wegmann, G., and Eppenberger, H. M. (1986) *J. Muscle Res. Cell Motil.* **7,** 25–34
12. Wallimann, T., Wegmann, G., Moser, H., Huber, R., and Eppenberger, H. M. (1986) *Proc. Natl. Acad. Sci. U. S. A.* **83,** 3816–3819
13. Turner, D. C., Wallimann, T., and Eppenberger, H. M. (1973) *Proc. Natl. Acad. Sci. U. S. A.* **70,** 702–705
14. Wallimann, T., Turner, D. C., and Eppenberger, H. M. (1977) *J. Cell Biol.* **75,** 297–317
15. Wallimann, T., and Eppenberger, H. M. (1985) in *Cell and Muscle Motility* (Shay, J. W., ed) Vol. 6, pp. 239–285, Plenum Publishing Corp., New York
16. Wallimann, T., Walzthöny, D., Wegmann, G., Moser, H., Eppenberger, H. M., and Barrantes, F. J. (1985) *J. Cell Biol.* **100,** 1063–1072
17. Scholte, H. R., Weijers, P. J., and Wit-Peeters, E. M. (1973) *Biochim. Biophys. Acta* **291,** 764–773
18. Schlame, M., and Augustin, W. (1985) *Biomed. Biochim. Acta* **44,** 1083–1088
19. Saks, V. A., Rosenstraukh, L. V., Smirnov, V. N., and Chazov, E. I. (1978) *Can. J. Physiol. Pharmacol.* **56,** 691–706
20. Jacobus, W. E. (1985) *Annu. Rev. Physiol.* **4,** 707–725
21. Bessman, S. P., and Geiger, P. J. (1981) *Science* **211,** 448–452
22. Bessmann, S. P., and Carpenter, Ch. L. (1985) *Annu. Rev. Biochem.* **54,** 831–862
23. Yang, W. C. T., Geiger, P. J., and Bessmann, S. P. (1977) *Biochem. Biophys. Res. Commun.* **76,** 882–887
24. Saks, V. A., Kupriyanov, V. V., Elizarova, G. V., and Jacobus, W. E. (1980) *J. Biol. Chem.* **255,** 755–763
25. Gellerich, F., and Saks, V. A. (1982) *Biochem. Biophys. Res. Commun.* **105,** 1473–1481
26. Moreadith, R. W., and Jacobus, W. E. (1982) *J. Biol. Chem.* **257,** 899–905
27. Wallimann, T. (1975) Ph.D. thesis No. 5437, Eidgenössische Technische Hochschule Zürich, Switzerland
28. Wallimann, T., Zurbriggen, B., Walzthöny, D., Eppenberger, H. M., Schnyder, Th., Lustig, A., and Engel, A. (1986) *J. Muscle Res. Cell Motil.* **7,** 72 (Abstr.)
29. Schnyder, Th., Schlegel, J., Engel, A., Eppenberger, H. M., Gross, H., and Wallimann, T. (1987) *Abstract of the 9th International Biophysical Congress,* August 23–28, Jerusalem, Israel

30. Roberts, R., and Grace, A. M. (1980) *J. Biol. Chem.* **255,** 2870–2877
31. Hexner, P. E., Radford, L. E., and Beams, J. W. (1961) *Proc. Natl. Acad. Sci. U. S. A.* **47,** 1848–1852
32. Engel, A. (1978) *Ultramicroscopy* **3,** 273–281
33. Walzthöny, D., Bähler, M., Eppenberger, H. M., Wallimann, T., and Engel, A. (1984) *EMBO J.* **3,** 2621–2626
34. Engel, A., Christen, F., and Michel, B. (1981) *Ultramicroscopy* **7,** 45–54
35. Kaper, J. M. (1968) in *Molecular Basis of Virology* (Fraenkel-Conrat, H., ed) pp. 1–133, Van Nostran-Reinhold, New York
36. Bevington, P. R. (1969) in *Data Reduction and Error Analysis for the Physical Science*, pp. 204–246, McGraw-Hill Publishers, New York
37. Reimer, L., Volbert, B., and Bracker, P. (1978) *Scanning* **1,** 233–242
38. Saxton, W. O., Pitt, T. J., and Horner, M. (1979) *Ultramicroscopy* **4,** 343–354
39. Bloomfield, V., VanHolde, K. E., and Dalton, W. O. (1967) *Biopolymers* **5,** 149–159
40. Jacobs, H. K., and Graham, M. (1978), *Fed. Proc.* **37,** (6) (Abstr.)
41. Grace, A. M., Perryman, M. B., and Roberts, R. (1983) *J. Biol. Chem.* **258,** 15346–15354
42. Schlegel, J., Schürch, U., Wyss, M., Eppenberger, H. M., and Wallimann, T. (1987) *Experientia* **43,** 678 (Abstr.)
43. Schlegel, J., Wyss, M., Schürch, U., Schnyder, Th., Quest, A., Wegmann, G., Eppenberger, H. M., and Wallimann, T. (1988) *J. Biol. Chem.* **263,** 16963–16969
44. Saks, V. A., Kuznetsov, A. V., Kupriyanov, V. V., Miceli, M. V., and Jacobus, W. E. (1985) *J. Biol. Chem.* **260,** 7757–7764
45. Nunally, R. L., and Hollis, D. P. (1979) *Biochemistry* **18,** 3642–3646
46. Barbour, R. L., Sotak, C. H. H., Levy, G. C., and Chan, S. H. P. (1984) *Biochemistry* **23,** 6053–6062
47. Barbour, R. L., Ribaudo, J., and Chan, S. H. P. (1984) *J. Biol. Chem.* **259,** 8246–8251
48. Murphy, E., Gabel, S. A., Funk, A., and London, R. E. (1988) *Biochemistry* **27,** 526–528
49. Degani, H., Laughlin, M., Campbell, S., and Shulman, R. G. (1985) *Biochemistry* **24,** 5510–5516
50. Toyo-oka, T., Nagayama, K., Umeda, M., Eguchi, K., and Hoseda, S. (1986) *Biochem. Biophys. Res. Commun.* **135,** 808–815
51. Hitzig, B. M. Prichard, J. W., Kantor, H. L., Ellington, W. R., Ingwall, J. S., Burt, C. T., Helman, S. I., and Koutcher, J. (1987) *FASEB J.* **1,** 22–31
52. Miller, D. S., and Horowitz, S. B. (1986) *J. Biol. Chem.* **261,** 13911–13915
53. Mahler, M. (1985) *J. Gen. Physiol.* **86,** 135–165
54. Gellerich, F. N., Schlame, M., Bohnensack, R., and Kunz, W. (1987) *Biochim. Biophys. Acta* **890,** 117–126
55. Zahler, R., Bittl, J., and Ingwall, J. S. (1987) *Biophys. J.* **51,** 883–893
56. Saks, V. A. Khuchua, Z. A., and Kuznetsov, A. V. (1987) *Biochim. Biophys. Acta* **891,** 138–144
57. Erickson-Viitanen, S., Geiger, P. J., Viitanen, P., and Bessman, S. P. 1982) *J. Biol. Chem.* **257,** 14405–14411
58. Brooks, S., and Suelter, C. H. (1987) *Arch. Biochem. Biophys.* **257,** 144–153
59. Adams, V., Bosch, W., Schlegel, J., Wallimann, T., and Brdiczka, D. (1988) *Biochim. Biophys. Acta,* in press
60. Marcillat, O., Goldschmidt, D., Eichenberger, D., and Vial, C. (1987) *Biochem. Biophys. Acta* **890,** 233–241
61. Müller, M., Moser, R., Cheneval, D., and Carafoli, E. (1985) *J. Biol. Chem.* **260,** 3839–3843
62. Peitsch, M. C., Tschopp, J., Kress, A., and Isliker, H. (1988) *Biochem. J.* **249,** 495–500
63. Beyer, K., and Klingenberg, M. (1985) *Biochemistry* **24,** 8321–8326
64. Knoll, G., and Brdiczka, D. (1983) *Biochim. Biophys. Acta* **733,** 102–110
65. Kuznetsov, A. V., and Saks, V. A. (1986) *Biochim. Biophys. Res. Commun.* **134,** 359–366
66. Hall, N., and DeLuca, M. (1984) *Arch. Biochem. Biophys.* **229,** 477–482
67. Lipskaya, T. Yu., and Rybina, I. V. (1987) *Biochemistry USSR* **52,** 690–700
68. Saks, V. A., Khuchua, Z. A., Kuznetsov, A. V., Veksler, V. I., and Sharov, V. G. (1986) *Biochem. Biophys. Res. Commun.* **139,** 1262–1271
69. Vial, C., Marcillat, O., Goldschmidt, D., and Eichenberger, D. (1986) *J. Mol. Cell Cardiol.* **18,** (Suppl. 2) (Abstr. 10)
70. Meyer, R. A. (1988) *Am. J. Physiol.* **254,** C548–553
71. Wallimann, T., Schlösser, T., and Eppenberger, H. M. (1984) *J. Biol. Chem.* **259,** 5238–5246
72. Ventura-Clapier, R., Saks, V. A., Vassort, G., Lauer, C., and Elizarova, G. V. (1987) *Am. J. Physiol.* **253,** C444–C555
73. Ventura-Clapier, R., Mekhefi, H., and Vassort, G. (1987) *J. Gen. Physiol.* **89,** 815–837
74. Brdiczka, D., Adams, V., Kottke, M., and Benz, R. (1989) *Proceedings of the International Conference on Anion Carriers of Mitochondrial Membranes.* Springer, Heidelberg BRD, in press
75. Kottke, M., Adams, V., Riesinger, I., Bremm, G., Bosch, W., Brdiczka, D., Sandri, G., and Panfili, E. (1988) *Biochim. Biophys. Acta* **935,** 82–102
76. Tanford, C. (1961) *Physical Chemistry of Macromolecules,* J. Wiley & Sons Inc., New York
77. Yue, R. H., Palmieri, R. H., Olson, O. E., and Kuby, S. A. (1967) *Biochemistry* **6,** 3204–3227
78. Schnyder, T., Engel, A., Gross, H., Eppenberger, M. M., and Wallimann, T. (1988) *Second International Symposium of the European Biophysical Society Association,* September 4–8, 1988 Springer-Verlag, Gwatt, Switzerland, in press